ELSEVIER

Energy Conversion and Management 45 (2004) 2297–2312

ENERGY CONVERSION & MANAGEMENT

www.elsevier.com/locate/enconman

Robust decentralized AGC in a restructured power system

H. Bevrani [a,*], Y. Mitani [b], K. Tsuji [a]

[a] Department of Electrical Engineering, Osaka University, 2-1 Yamada-Oka, Suita, Osaka 565-0871, Japan
[b] Department of Electrical Engineering, Kyushu Institute of Technology, Kyushu, Japan

Received 11 September 2003; accepted 23 November 2003
Available online 24 January 2004

Abstract

This paper addresses a new decentralized robust strategy to adapt the well tested classical automatic generation control (AGC) system to the changing environment of power system operation under deregulation based on the bilateral AGC scheme. In each control area, the effect of bilateral contracts is taken into account in a modified traditional dynamical model as a set of new input signals. The AGC problem is formulated as a multi-objective control problem, and the mixed H_2/H_∞ control technique is used to synthesis the desired robust controllers for AGC design in a multi-area power system.

A three area power system example with possible contract scenarios and a wide range of load changes is given to illustrate the proposed approach. The results of the proposed control strategy are compared with the pure H_∞ method. The resulting controllers are shown to minimize the effect of disturbances and maintain robust performance.

Keywords: Automatic generation control; Mixed H_2/H_∞ control; Restructured power system; Linear matrix inequalities; Bilateral contracts

1. Introduction

Currently, the electric power industry is in transition from large, vertically integrated utilities providing power at regulated rates to an industry that will incorporate competitive companies selling unbundled power at lower rates. In a deregulated environment, automatic generation

* Corresponding author. Tel.: +81-6-6879-7712; fax: +81-6-6879-7713.
E-mail address: bevrani@polux.pwr.eng.osaka-u.ac.jp (H. Bevrani).

0196-8904/$ - see front matter © 2003 Elsevier Ltd. All rights reserved.
doi:10.1016/j.enconman.2003.11.018

control (AGC) acquires a fundamental role to enable power exchanges and to provide better conditions for electricity trading. AGC is treated as an ancillary service that is essential for maintaining the electrical system reliability at an adequate level [1].

In an open energy market, generation companies (Gencos) may or may not participate in the AGC task. On the other hand, a distribution company (Disco) may contract individually with a Genco or independent power producers (IPPs) for power in its area or other areas. Currently these transactions are done under the supervision of the independent system operator (ISO), independent contract administrator (ICA) or other responsible organizations.

Several control scenarios based on robust and optimal approaches have been proposed for the AGC system in deregulated power systems. Some research works are contained in Refs. [2–13]. Recently, several reported strategies attempted to adapt well tested classical AGC schemes to the changing environment of power system operation under deregulation [14–17]. The main advantage of these strategies is in using the basic concepts of the traditional framework and avoiding use of impractical or untested AGC models.

Following the mentioned attempts, this paper addresses a novel control strategy using a modified AGC system. The AGC goals, i.e. frequency regulation and tracking the load changes, maintaining the tie line power interchanges to specified values and considering the generation rate limits, determines the AGC synthesis as a multi-objective control problem. In most reported robust AGC approaches, only one single norm is used to capture design specifications. It is clear that meeting all the AGC design objectives by a single control approach with regard to the increasing complexity and changing of power system structure is difficult. Furthermore, each robust method is mainly useful to capture a set of special specifications. For instance, the regulation against random disturbances more naturally can be addressed by LQG or H_2 synthesis, while the H_∞ approach is more useful for holding closed loop stability and formulation of physical control constraints. It is shown that using the combination of H_2 and H_∞ (mixed H_2/H_∞) allows a better performance for a control design problem including both sets of the above objectives [18–20].

In this paper, first we introduce a modified dynamical model for a general control area in the deregulated environment, following the ideas presented in [15–17]. This model shows how the bilateral contracts are incorporated in the traditional AGC system, leading to a new model. Then, the AGC problem will be formulated as a multi-objective control problem and solved by the mixed H_2/H_∞ control approach to obtain the desired robust decentralized controllers. We applied the proposed strategy to a three control area example. The results show that the controllers guarantee robust performance for a wide range of operating conditions. The results of the proposed multi-objective approach are compared with those of the pure H_∞ controllers (using the general LMI technique), which show the effectiveness of this approach.

This paper is organized as follows. Section 2 describes the modified traditional AGC structure versus the new environment. Technical background on the mixed H_2/H_∞ control approach is given in Section 3. Section 4 presents the problem formulation and synthesis framework for a given control area. The proposed methodology and pure H_∞ control design are applied to a three area power system as a case study in Section 5. Finally, to demonstrate the effectiveness of the proposed method, some simulation results for a set of various contract scenarios are given in Section 6.

2. Modified traditional AGC structure

The traditional AGC is well discussed in Refs. [21,22]. In a traditional power system structure, the generation, transmission and distribution is owned by a single entity called a vertically integrated utility (VIU), which supplies power to the customers at regulated rates. All such control areas are interconnected by tie lines. Following a load disturbance within an area, the frequency of that area experiences a transient change, and the feedback mechanism comes into play and generates an appropriate rise/lower signal to the turbine to make the generation follow the load. In steady state, the generation is matched with the load, driving the tie line power and frequency deviations to zero [17].

In the restructured power systems, the VIU no longer exists, however, the common objectives, i.e. restoring the frequency and the net interchanges to their desired values for each control area are remained. In the vertically integrated power system structure, it is assumed that each bulk generator unit is equipped with secondary control and frequency regulation requirements, but in an open energy market, Gencos may or may not participate in the AGC problem. Therefore, in a control area including numerous distributed generators with an open access policy and a few AGC participators, there comes the need for novel model and efficient control strategies to maintain reliability and eliminate the frequency error. Here, we introduce a modified dynamical model for the traditional AGC system by taking into account the effect of bilateral contracts on the dynamics, following the ideas presented in Refs. [15–17]. In Ref. [17], a traditional based dynamical model is proposed for a two control area in a deregulated environment. We have generalized this idea for a multi-area power system. The new AGC model will need all the information required in a vertically integrated utility industry plus the contract data information.

The new power system structure includes separate generation, transmission and distribution companies with an open access policy. Based on bilateral transactions, a Disco has the freedom to contract with any available Genco in its own or another control area. Therefore, the concept of physical control area is replaced by a virtual control area (VCA). The boundary of the VCA is flexible and encloses the Gencos and the Disco associated with the contract.

For simplicity, analogously to the traditional AGC, the physical control area boundaries are assumed for each Disco, its distribution area and the local Gencos as before. However, the Disco may have a contract with a Genco outside its distribution area boundaries, in another control area. Similar to Ref. [2], the general theme in our work is that the loads (the Discos) are responsible for purchasing the services they require. Therefore, the overall power system structure can be considered as a collection of distribution areas (Discos) as separate control areas interconnected through high voltage transmission lines or tie lines. Each control area has its own AGC and is responsible for tracking its own load and honoring tie line power exchange contracts with its neighbours. All the transactions have to be cleared by the ISO or other responsible organizations. There can be various combinations of contracts between each Disco and the available Gencos. On the other hand, each Genco can contract with various Discos. Similar to the Disco participation matrix in Ref. [17], let us define the "generation participation matrix (GPM)" concept to visualize these bilateral contracts conveniently in the generalized model.

The GPM shows the participation factor of each Genco in the considered control areas and each control area is determined by a Disco. The rows of a GPM correspond to Gencos and the

columns to control areas that contract power. For example, for a large scale power system with m control area (Discos) and n Gencos, the GPM will have the following structure.

$$\mathrm{GPM} = \begin{bmatrix} \mathrm{gpf}_{11} & \mathrm{gpf}_{12} & \cdots & \mathrm{gpf}_{1(m-1)} & \mathrm{gpf}_{1m} \\ \mathrm{gpf}_{21} & \mathrm{gpf}_{22} & \cdots & \mathrm{gpf}_{2(m-1)} & \mathrm{gpf}_{2m} \\ \vdots & \vdots & \vdots & \vdots & \vdots \\ \mathrm{gpf}_{(n-1)1} & \mathrm{gpf}_{(n-1)2} & \cdots & \mathrm{gpf}_{(n-1)(m-1)} & \mathrm{gpf}_{(n-1)m} \\ \mathrm{gpf}_{n1} & \mathrm{gpf}_{n2} & \cdots & \mathrm{gpf}_{n(m-1)} & \mathrm{gpf}_{nm} \end{bmatrix} \tag{1}$$

where gpf_{ij} refers to "generation participation factor" and shows the participation factor of Genco i in the load following of area j (based on a specified bilateral contract). The sum of all the entries in a column in this matrix is unity, i.e.

$$\sum_{i=1}^{n} \mathrm{gpf}_{ij} = 1 \tag{2}$$

Any entry in a GPM that corresponds to a contracted load by a Disco, demanded from the corresponding Genco, must be reflected to the control area system. This introduces new information signals that were absent in the traditional AGC structure. These signals identify that Genco has to follow a load demanded by which Disco. The scheduled flow over the tie lines must be adjusted by demand signals of those distribution control areas having a contract with Gencos outside its boundaries. The difference between scheduled and current (actual) tie line power flows gives a tie line power error which is used to compose an area control error (ACE) signal.

Based on the above explanations, the modified AGC block diagram for control area i will be obtained in a deregulated environment as shown in Fig. 1. New information signals due to various

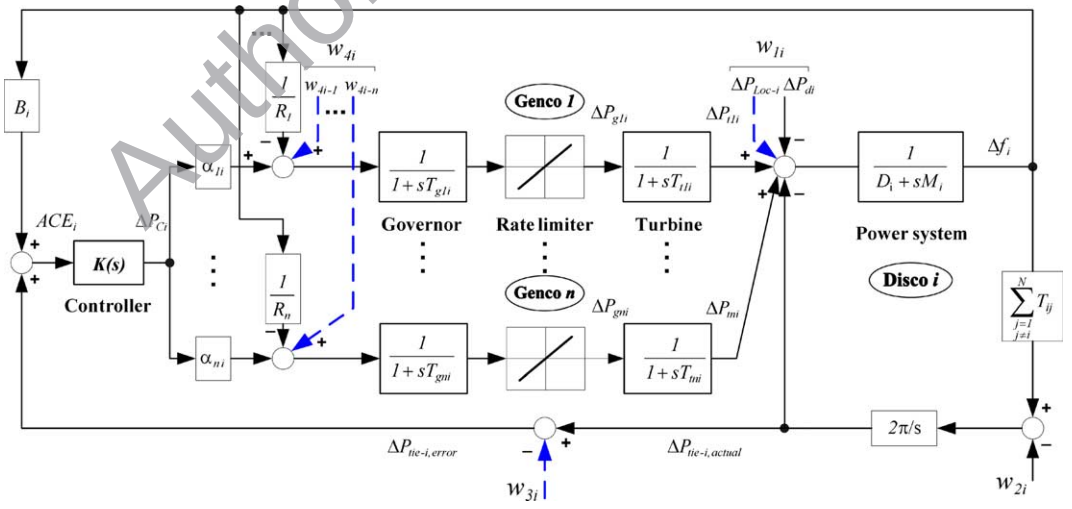

Fig. 1. Modified control area in a deregulated environment.

possible contracts between Disco i and other Discos and Gencos are shown as dashed line inputs. Where,

Δf_i frequency deviation,
ΔP_{gi} governor valve position,
ΔP_{ci} governor load set point,
ΔP_{ti} turbine power,
ΔP_{tie-i} net tie line power flow,
ΔP_{di} area load disturbance,
M_i equivalent inertia constant,
D_i equivalent damping coefficient,
T_{gi} governor time constant,
T_{ti} turbine time constant,
T_{ij} tie line synchronizing coefficient between areas i and j,
B_i frequency bias,
R_i drooping characteristic,
α ACE participation factor,
N number of control areas,
ΔP_{Lj} contracted demand of area j,
ΔP_{Loc-i} contracted/uncontracted local demand in area i,
w_{3i} scheduled ΔP_{tie-i} ($\Delta P_{tie-i,scheduled}$),
$\Delta P_{tie-i,actual}$ actual ΔP_{tie-i} and

$$w_{1i} = \Delta P_{Loc-i} + \Delta P_{di} \tag{3}$$

$$w_{2i} = \sum_{\substack{j=1 \\ j\neq i}}^{N} T_{ij}\Delta f_j \tag{4}$$

$$\sum_{k=1}^{n} \alpha_{ki} = 1 \tag{5}$$

$$0 \leqslant \alpha_{ki} \leqslant 1 \tag{6}$$

Based on the given idea in Ref. [17], we can generalize the scheduled ΔP_{tie-i} (w_{3i}) for a N control area power system as follows.

$$w_{3i} = \sum(\text{Total export power} - \text{Total import power})$$

$$= \sum_{\substack{j=1 \\ j\neq i}}^{N} \left(\sum_{k=1}^{n} \text{gpf}_{kj} \right) \Delta P_{Lj} - \sum_{k=1}^{n} \left(\sum_{\substack{j=1 \\ j\neq i}}^{N} \text{gpf}_{jk} \right) \Delta P_{Li} \tag{7}$$

According to Fig. 1, we can write

$$\Delta P_{tie-i,error} = \Delta P_{tie-i,actual} - w_{3i} \tag{8}$$

and the elements of vector w_{4i} can be expressed as,

$$\begin{aligned} w_{4i-1} &= \textstyle\sum_{j=1}^{N} \mathrm{gpf}_{1j}\Delta P_{\mathrm{L}j} \\ &\vdots \\ w_{4i-n} &= \textstyle\sum_{j=1}^{N} \mathrm{gpf}_{nj}\Delta P_{\mathrm{L}j} \end{aligned} \tag{9}$$

The generation of each Genco must track the contracted demands of Discos in steady state. The desired total power generation of a Genco i in terms of GPM entries can be calculated as

$$\Delta P_{mi} = \sum_{j=1}^{N} \mathrm{gpf}_{ij}\Delta P_{\mathrm{L}j} \tag{10}$$

In order to take into account the contract violation cases, like as Ref. [15], the excess demand by a distribution area (Disco) is not contracted out to any Genco and the load change in the area appears only in terms of its ACE and is shared by all the Gencos of the area (in which the contract violation occurs).

3. Mixed H_2/H_∞: technical background

In many real world control problems, we are simultaneously following several objectives, such as stability, disturbance attenuation and reference tracking and considering the practical constraints. Pure H_∞ synthesis cannot adequately capture all design specifications. For example, H_∞ synthesis mainly enforces closed loop stability and meeting some constraints and limitations, while noise attenuation or regulation against random disturbances are more naturally expressed in LQG terms (H_2 synthesis). Mixed H_2/H_∞ control synthesis gives a powerful multi-objective design addressed by the LMI techniques. This section gives a brief overview of mixed H_2/H_∞ output feedback control design.

The general synthesis control scheme is shown in Fig. 2. $G(s)$ is a linear time invariant system with the following state space realization

$$\begin{aligned} \dot{x} &= Ax + B_1 w + B_2 u \\ z_\infty &= C_\infty x + D_{\infty 1} w + D_{\infty 2} u \\ z_2 &= C_2 x + D_{21} w + D_{22} u \\ y &= C_y x + D_{y1} w \end{aligned} \tag{11}$$

where x is the state variable vector, w is the disturbance and other external input vectors and y is the measured output vector. The output channel z_2 is associated with the LQG aspects (H_2 performance) while the output channel z_∞ is associated with the H_∞ performance. Let $T_\infty(s)$ and $T_2(s)$ be the transfer functions from w to z_∞ and z_2, respectively, and consider the following state space realization for a closed loop system.

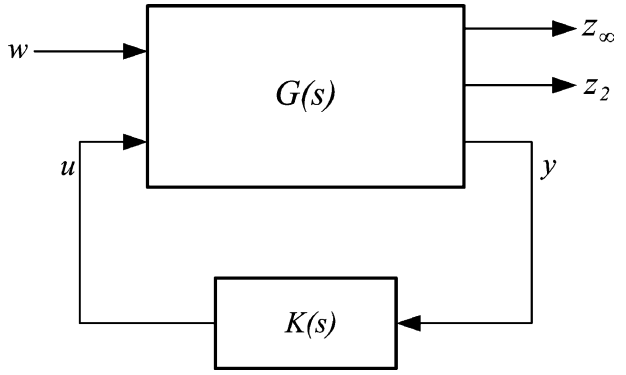

Fig. 2. Closed loop system via mixed H_2/H_∞ control.

$$\begin{aligned}\dot{x}_{cl} &= A_{cl}x_{cl} + B_{cl}w\\ z_\infty &= C_{cl1}x_{cl} + D_{cl1}w\\ z_2 &= C_{cl2}x_{cl} + D_{cl2}w\end{aligned} \tag{12}$$

The following lemmas express the design objectives in term of LMIs [23]. Interested readers can find more details in Refs. [18–20].

Lemma 1 (H_∞ performance)**.** *The closed loop RMS gain for $T_\infty(s)$ does not exceed γ_∞ if and only if there exists a symmetric matrix $X_\infty > 0$ such that*

$$\begin{bmatrix} A_{cl}X_\infty + X_\infty A_{cl}^T & B_{cl} & X_\infty C_{cl1}^T \\ B_{cl}^T & -I & D_{cl1}^T \\ C_{cl1}X_\infty & D_{cl1} & -\gamma_\infty^2 I \end{bmatrix} < 0 \tag{13}$$

Lemma 2 (H_2 performance)**.** *The H_2 norm of $T_2(s)$ does not exceed γ_2 if and only if $D_{cl2} = 0$ and there exist two symmetric matrices X_2 and Q such that*

$$\begin{bmatrix} A_{cl}X_2 + X_2A_{cl}^T & B_{cl} \\ B_{cl}^T & -I \end{bmatrix} < 0, \quad \begin{bmatrix} Q & C_{cl2}X_2 \\ X_2C_{cl2}^T & X_2 \end{bmatrix} > 0, \quad \mathrm{Trace}(Q) < \gamma_2^2 \tag{14}$$

The mixed H_2/H_∞ control design method uses both lemmas and gives us an output feedback controller $K(s)$ that minimizes a trade off criterion of the form

$$k_1\|T_\infty(s)\|_\infty^2 + k_2\|T_2(s)\|_2^2 \quad (k_1 \geqslant 0,\ k_2 \geqslant 0) \tag{15}$$

An efficient algorithm for solving this problem is available in function *hinfmix* of the LMI control toolbox for Matlab [23].

4. Problem formulation and proposed control framework

A large scale power system consists of a number of interconnected distribution control areas; each control area may have several Gencos (Fig. 1). The main control framework, in order to formulation the AGC problem via a mixed H_2/H_∞ control design, for a given control area is shown in Fig. 3. $G_i(s)$ denotes the dynamical model corresponding to the modified control area shown in Fig. 1. According to Eqs. (11), the state space model for control area i can be obtained as

$$\begin{aligned} \dot{x}_i &= A_i x_i + B_{1i} w_i + B_{2i} u_i \\ z_{\infty i} &= C_{\infty i} x_i + D_{\infty 1i} w_i + D_{\infty 2i} u_i \\ z_{2i} &= C_{2i} x_i + D_{21i} w_i + D_{22i} u_i \\ y_i &= C_{yi} x_i + D_{y1i} w_i \end{aligned} \tag{16}$$

where

$$x_i^{\mathrm{T}} = [\,\Delta f_i \quad \Delta P_{\mathrm{tie}-i} \quad x_{\mathrm{t}i} \quad x_{\mathrm{g}i}\,] \tag{17}$$

$$x_{\mathrm{t}i} = [\,\Delta P_{\mathrm{t}1i} \quad \Delta P_{\mathrm{t}2i} \quad \cdots \quad \Delta P_{\mathrm{t}ni}\,] \tag{18}$$

$$x_{\mathrm{g}i} = [\,\Delta P_{\mathrm{g}1i} \quad \Delta P_{\mathrm{g}2i} \quad \cdots \quad \Delta P_{\mathrm{g}ni}\,] \tag{19}$$

$$u_i = \Delta P_{Ci}, \quad y_i = \beta_i \Delta f_i + \Delta P_{\mathrm{tie}-i} - w_{3i} \tag{20}$$

$$z_{\infty i} = \eta_{1i} \Delta P_{Ci} = \eta_{1i} u_i, \quad z_{2i}^{\mathrm{T}} = [\,\eta_{2i} \Delta f_i \quad \eta_{3i} \Delta P_{\mathrm{tie}-i}\,] \tag{21}$$

$$w_i^{\mathrm{T}} = [\,w_{1i} \quad w_{2i} \quad w_{3i} \quad w_{4i}\,], \quad w_{4i}^{\mathrm{T}} = [\,w_{4i-1} \quad w_{4i-2} \quad \cdots \quad w_{4i-n}\,] \tag{22}$$

and

$$A_i = \begin{bmatrix} A_{i11} & A_{i12} & A_{i13} \\ A_{i21} & A_{i22} & A_{i23} \\ A_{i31} & A_{i32} & A_{i33} \end{bmatrix}, \quad B_{1i} = \begin{bmatrix} B_{1i11} & B_{1i12} \\ B_{1i21} & B_{1i22} \\ B_{1i31} & B_{1i32} \end{bmatrix}, \quad B_{2i} = \begin{bmatrix} B_{2i1} \\ B_{2i2} \\ B_{2i3} \end{bmatrix}$$

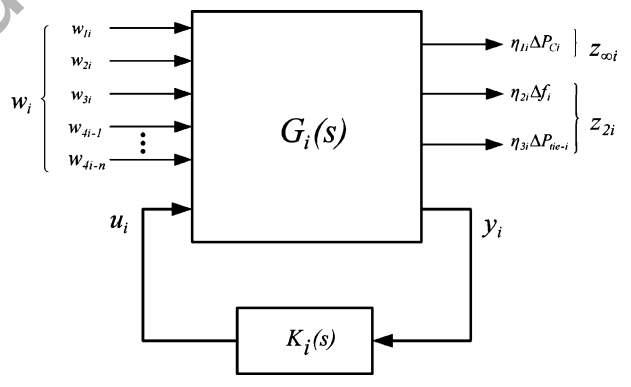

Fig. 3. Proposed control framework.

$$c_{2i} = \begin{bmatrix} \eta_{1i} & 0 & 0_{1\times 2n} \\ 0 & \eta_{2i} & 0_{1\times 2n} \end{bmatrix}, \quad D_{21i} = 0_{2\times(n+3)}, \quad D_{22i} = 0_{2\times 1}$$

$$C_{\infty i} = 0_{1\times(2n+2)}, \quad D_{\infty 1i} = 0_{1\times(n+3)}, \quad D_{\infty 2i} = \eta_{3i}$$

$$c_{yi} = [\,\beta_i \quad 1 \quad 0_{1\times 2n}\,], \quad D_{y1i} = [\,0 \quad 0 \quad -1 \quad 0_{1\times n}\,]$$

$$A_{i11} = \begin{bmatrix} -D_i/M_i & -1/M_i \\ 2\pi \sum_{\substack{j=1 \\ j\neq i}}^{N} T_{ij} & 0 \end{bmatrix}, \quad A_{i12} = \begin{bmatrix} 1/M_i & \cdots & 1/M_i \\ 0 & \cdots & 0 \end{bmatrix}_{2\times n}$$

$$A_{i22} = -A_{i23} = \mathrm{diag}[\,-1/T_{\mathrm{t}1i} \quad -1/T_{\mathrm{t}2i} \quad \cdots \quad -1/T_{\mathrm{t}ni}\,]$$

$$A_{i33} = \mathrm{diag}[\,-1/T_{\mathrm{g}1i} \quad -1/T_{\mathrm{g}2i} \quad \cdots \quad -1/T_{\mathrm{g}ni}\,]$$

$$A_{i31} = \begin{bmatrix} -1/(T_{\mathrm{g}1i}R_{1i}) & 0 & 0 \\ \vdots & \vdots & \vdots \\ -1/(T_{\mathrm{g}ni}R_{ni}) & 0 & 0 \end{bmatrix}, \quad A_{i13} = A_{i21}^{\mathrm{T}} = 0_{2\times n}, \quad A_{i32} = 0_{n\times n}$$

$$B_{1i11} = \begin{bmatrix} -1/M_i & 0 & 0 \\ 0 & -2\pi & 0 \end{bmatrix}, \quad B_{1i21} = B_{1i31} = 0_{n\times 2}, \quad B_{1i12} = 0_{2\times n}, \quad B_{1i22} = 0_{n\times n},$$

$$B_{1i32} = \mathrm{diag}[\,1/T_{\mathrm{g}1i} \quad 1/T_{\mathrm{g}2i} \quad \cdots \quad 1/T_{\mathrm{g}ni}\,], \quad B_{2i1} = 0_{2\times 1}, \quad B_{2i2} = 0_{n\times 1},$$
$$B_{2i3}^{\mathrm{T}} = [\,\alpha_{1i}/T_{\mathrm{g}1i} \quad \alpha_{2i}/T_{\mathrm{g}2i} \quad \cdots \quad \alpha_{ni}/T_{\mathrm{g}ni}\,]$$

The H_∞ performance is used to set a limit on the control set point to penalize the fast change and large over shoot in the control action signal. The H_2 performance is used to minimize the effects of disturbances on the control area frequency and tie line flow signals. Therefore, it is expected that the proposed strategy will satisfy the main objectives of the AGC system under load change and bilateral contracts variation. The η_{1i}, η_{2i} and η_{3i} in Fig. 3 and Eqs. (21) are constant weighting coefficients that are chosen by the designer to get the desired performance. In the next section, two sets of robust controllers are developed for a power system example including three control areas. The first one, includes pure H_∞ controllers based on the general LMI technique, and the second one contains designed low order controllers based on the proposed mixed H_2/H_∞ approach (described in Section 3) with the same assumed objectives to achieve desired robust performance.

5. Case study

To illustrate the effectiveness of the modelling strategy and proposed control design, a three control area power system, shown in Fig. 4, is considered as a test system. It is assumed that each control area includes two Gencos and one Disco. The power system parameters are tabulated in Tables 1 and 2.

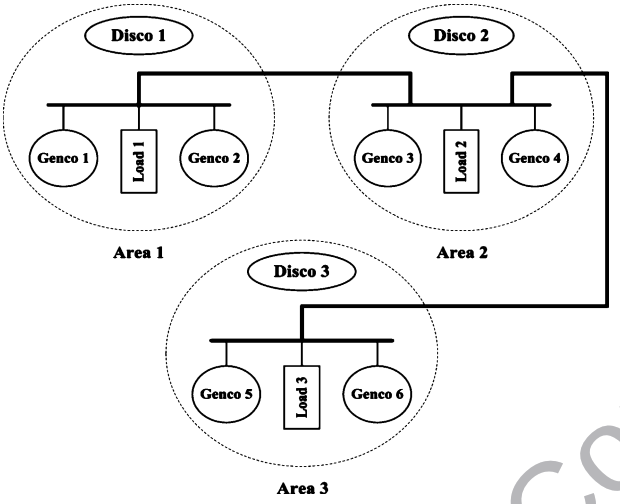

Fig. 4. Three control area power system.

Table 1
Applied data for Gencos

Quantity	Genco 1	Genco 2	Genco 3	Genco 4	Genco 5	Genco 6
Rate (MW)	800	1000	1100	1200	1000	1000
R (Hz/pu)	2.4	3.3	2.5	2.4	3	2.4
T_t (s)	0.36	0.42	0.44	0.4	0.36	0.4
T_g (s)	0.06	0.07	0.06	0.08	0.07	0.08
α	0.5	0.5	0.5	0.5	0.5	0.5

Table 2
Applied control area parameters

Quantity	Area 1	Area 2	Area 3
D (pu/Hz)	0.0084	0.014	0.011
M (pu s)	0.1667	0.2	0.1667
B (pu/Hz)	0.8675	0.795	0.870
T_{ij} (pu/Hz)	$T_{12} = T_{23} = 0.545$		

5.1. Pure H_∞ control design

In order to compare, for each area, in addition to the proposed control strategy, a pure H_∞ dynamic output feedback controller is developed using Lemma 1. Specifically, the control design is reduced to an LMI formulation, and then, the H_∞ control problem is solved according to the LMI constraint (13) using the function *hinflmi* provided by MATLAB's LMI control toolbox [23]. This function gives an optimal H_∞ controller through minimizing the guaranteed robust per-

formance index subject to specified constraints and returns the controller $K(s)$ with optimal robust performance index.

The same control framework (shown in Fig. 3) is used for the pure H_∞ control design but using only one fictitious output channel (z_∞) as

$$z_\infty^{\mathrm{T}} = [\,\eta_{1i}\Delta P_{Ci} \quad \eta_{2i}\Delta f_i \quad \eta_{3i}\Delta P_{\mathrm{tie}-i}\,] \tag{23}$$

A set of suitable constant weights η_{1i}, η_{2i} and η_{3i} are chosen as 2.5, 1 and 1, respectively. The resulting controllers are the dynamic type and are given as follows, whose orders are the same as the size of the area model (here 6).

$$\begin{aligned}
K_{1\infty}(s) &= \frac{-4.3183s^5 - 151.5977s^4 - 1591.4874s^3 - 4630.9097s^2 - 3529.211s + 596.585}{s^6 + 42.6561s^5 + 645.1347s^4 + 4262.8509s^3 + 13116.3347s^2 + 16735.9031s + 5105.7057} \\
K_{2\infty}(s) &= \frac{-2.7694s^5 - 90.4397s^4 - 858.9605s^3 - 2067.3481s^2 - 668.8242s + 1214.4936}{s^6 + 39.4468s^5 + 545.6694s^4 + 3313.9408s^3 + 9898.8032s^2 + 14038.0905s + 7342.4697} \\
K_{3\infty} &= \frac{-4.5755s^5 - 141.8668s^4 - 1343.0582s^3 - 3781.6026s^2 - 2851.0296s + 366.7874}{s^6 + 38.9744s^5 + 552.8201s^4 + 3547.385s^3 + 10743.1064s^2 + 13506.6111s + 3887.5418}
\end{aligned} \tag{24}$$

5.2. Mixed H_2/H_∞ control design

At the next step, according to the synthesis methodology (mixed H_2/H_∞) described in Section 3, a set of three decentralized robust controllers is designed. The problem formulation and control framework are explained in Section 4. The constant weights are chosen to be the same as pure H_∞ design and both k_1 and k_2 in Eq. (15) are fixed as unity.

The order of the resulting controllers is 6. Using the standard Hankel norm approximation, the order is reduced to 3 for each controller with no performance degradation. For example, the Bode plot of the full order and reduced order controllers for areas 1 and 2 are shown in Fig. 5, which present the same frequency response for both the original and reduced order controllers. The transfer functions of the resulting reduced controllers with simple structures are

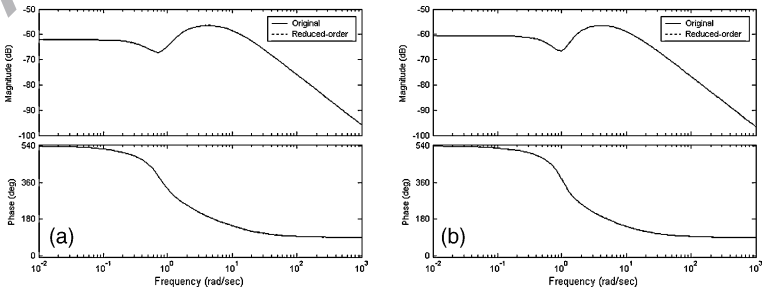

Fig. 5. Bode plots comparison of full order (original) and reduced controllers: (a) $K_{1\mathrm{mix}}(s)$, (b) $K_{2\mathrm{mix}}(s)$.

$$K_{1\text{mix}}(s) = \frac{-0.0161s^2 + 0.0099s - 0.0097}{s^3 + 10.9846s^2 + 21.5941s + 12.1933}$$
$$K_{2\text{mix}}(s) = \frac{-0.0147s^2 + 0.0092s - 0.0148}{s^3 + 10.17s^2 + 19.6734s + 15.478} \quad (25)$$
$$K_{3\text{mix}}(s) = \frac{-0.0167s^2 + 0.0107s - 0.0101}{s^3 + 12.1815s^2 + 24.9846s + 14.4173}$$

6. Simulation results

In order to demonstrate the effectiveness of the proposed strategy, some simulations were conducted. In these simulations, the proposed low order controllers, Eqs. (25), were applied to the three control area power system described in Fig. 4. The performance of the closed loop system using the proposed controllers in comparison with the designed full order pure H_∞ controllers, Eqs. (24), is tested for the various possible scenarios of bilateral contracts and load disturbances. Here, because of lack of space, the system responses are shown for two scenarios only, which include different bilateral contracts (GPM) and large load disturbances.

Scenario 1: It is assumed that a large load demand (as a step load disturbance) is requested in each control area:

$$\Delta P_{L1} = 100 \text{ MW}, \quad \Delta P_{L2} = 70 \text{ MW}, \quad \Delta P_{L3} = 60 \text{ MW}$$

Assume each Disco demand is sent to its local Gencos only, based on the following GPM

$$\text{GPM} = \begin{bmatrix} 0.5 & 0 & 0 \\ 0.5 & 0 & 0 \\ 0 & 0.5 & 0 \\ 0 & 0.5 & 0 \\ 0 & 0 & 0.5 \\ 0 & 0 & 0.5 \end{bmatrix}$$

The frequency deviation (Δf), power changes (ΔP_m) and area control error (ACE) of the closed loop system are shown in Fig. 6a–c. Using the proposed method, the area control error and frequency deviation of all the areas are quickly driven back to zero and the generated powers and tie line powers properly converge to specified values. As shown in these figures, the actual generated powers of the Gencos, according to Eq. (10), reach the desired values in the steady state.

$$\Delta P_{m1} = \text{gpf}_{11}\Delta P_{L1} + \text{gpf}_{12}\Delta P_{L2} + \text{gpf}_{13}\Delta P_{L3} = 0.5(0.1) + 0 + 0 = 0.05 \text{ pu}$$

and

$$\Delta P_{m2} = 0.05 \text{ pu}, \quad \Delta P_{m3} = \Delta P_{m4} = 0.035 \text{ pu}, \quad \Delta P_{m5} = \Delta P_{m6} = 0.03 \text{ pu}$$

Since there are no contracts between areas, the scheduled steady state power flows, Eq. (7), over the tie lines are zero. The actual tie line powers are shown in Fig. 6d. The difference between mixed H_2/H_∞ and pure H_∞ controllers will be clear if we apply a set of larger step disturbances under more complex bilateral contracts.

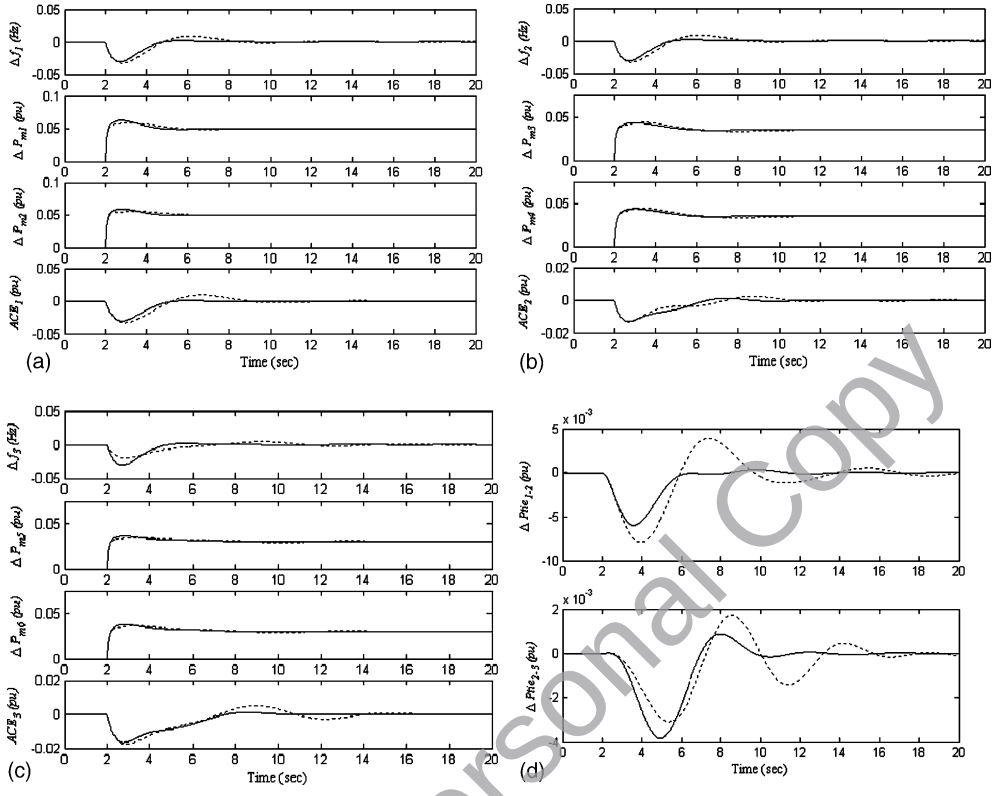

Fig. 6. Power system responses to scenario 1. Solid (mixed H_2/H_∞), dotted (H_∞): (a) area 1, (b) area 2, (c) area 3, and (d) tie line powers.

Scenario 2: Consider the following larger demands by Disco 2 and Disco 3,

$$\Delta P_{L1} = 100 \text{ MW}, \quad \Delta P_{L2} = 100 \text{ MW}, \quad \Delta P_{L3} = 100 \text{ MW}$$

and assume the Discos contract with the available Gencos in other areas according to the following GPM

$$\text{GPM} = \begin{bmatrix} 0.25 & 0.25 & 0 \\ 0.5 & 0 & 0 \\ 0 & 0.25 & 0.75 \\ 0.25 & 0.25 & 0 \\ 0 & 0.25 & 0 \\ 0 & 0 & 0.25 \end{bmatrix}$$

The closed loop responses for each area are shown in Fig. 7a–d. According to Eq. (10), the actual generated powers of the Gencos for this scenario can be obtained as

$$\Delta P_{m1} = 0.25(0.1) + 0.25(0.1) + 0 = 0.05 \text{ pu}$$

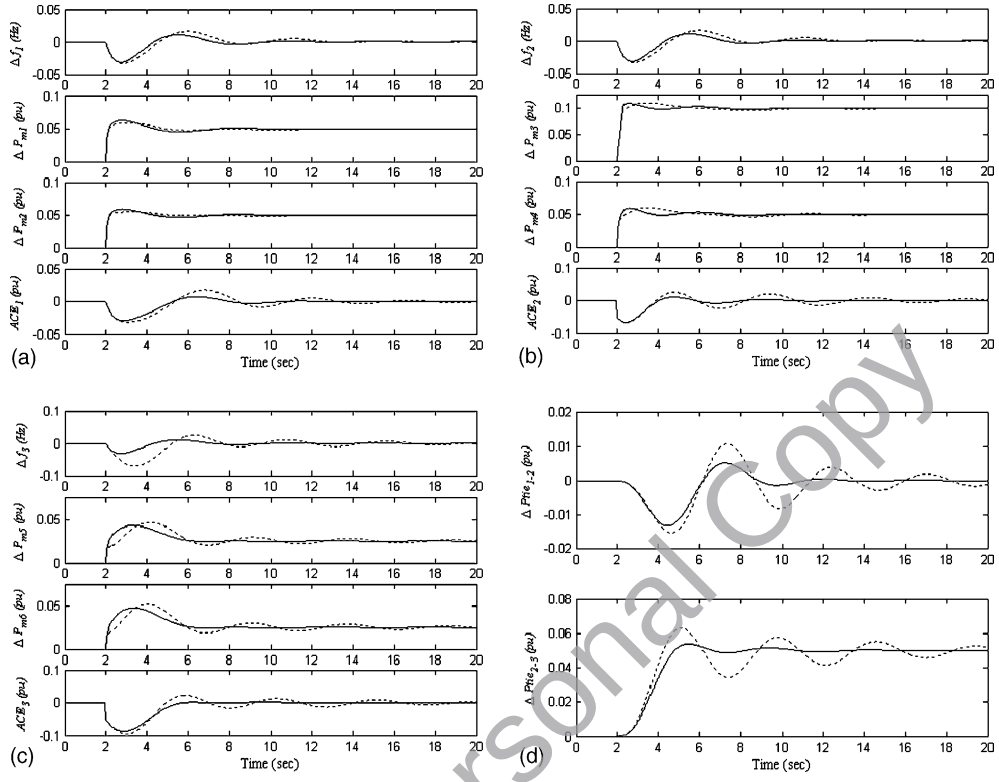

Fig. 7. Power system responses to scenario 2. Solid (mixed H_2/H_∞), dotted (H_∞): (a) area 1, (b) area 2, (c) area 3, and (d) tie line powers.

and

$$\Delta P_{m2} = 0.05 \text{ pu}, \quad \Delta P_{m3} = 0.1 \text{ pu}, \quad \Delta P_{m4} = 0.05 \text{ pu}, \quad \Delta P_{m5} = \Delta P_{m6} = 0.025 \text{ pu}$$

Also, the simulation results show the same values in steady state. The scheduled power tie lines in the directions from area 1 to area 2 and area 2 to area 3, using Eq. (7) are obtained as

$$\Delta P_{\text{tie},1\text{–}2} = (\text{gpf}_{12} + \text{gpf}_{22})\Delta P_{\text{L2}} - (\text{gpf}_{31} + \text{gpf}_{41})\Delta P_{\text{L1}} = (0.25 + 0)0.1 - (0 + 0.25)0.1 = 0 \text{ pu}$$
$$\Delta P_{\text{tie},2\text{–}3} = (0.75 + 0)0.1 - (0.25 + 0)0.1 = 0.05 \text{ pu}$$

Fig. 7d shows the actual tie line powers, and they reach the above values at steady state. The simulation results show the validity of the generalized AGC model and demonstrate that the proposed low order controllers perform robustness better than the full order H_∞ controllers for a wide range of load disturbances and possible bilateral contract scenarios.

7. Conclusion

In this paper, the AGC is considered as a multi-objective control problem and a new method for robust decentralized AGC design using a mixed H_2/H_∞ approach has been proposed for a

modified traditional AGC system model according to bilateral contracts in the restructured power system. The design strategy includes enough flexibility to set the desired level of performance and gives a set of simple controllers, which are commonly useful in real world power systems.

The proposed method was applied to a three control area power system and tested under various load scenarios. The results are compared with the results of applied pure H_∞ output controllers. The simulation results demonstrated the effectiveness of the methodology. It was shown that the designed controllers are capable to guarantee robust performance, such as precise reference frequency tracking and disturbance attenuation under a wide range of area load disturbances and possible contracted scenarios.

Acknowledgements

The authors are grateful to Dr. V. Donde from the University of Illinois (USA) and Prof. M. Ikeda from Osaka University (Japan) for their kind discussions.

References

[1] Jaleeli N, Ewart DN, Fink LH. Understanding automatic generation control. IEEE Trans Power Syst 1999;7(3):1106–22.
[2] Chritie RD, Bose A. Load–frequency control issues in power system operation after deregulation. IEEE Trans Power Syst 1996;11(3):1191–200.
[3] Meliopouls APS, Cokkinides GJ, Bakirtzis AG. Load–frequency control service in a deregulated environment. In: Proceedings of 31st International Conference on System Sciences, USA, 1998. p. 24–31.
[4] Bevrani H. Robust load–frequency controller in a deregulated environment: a μ-synthesis approach. In: Proceedings of IEEE International Conference on Control Applications, USA, 1999. p. 616–21.
[5] Feliachi A. Reduced H_∞ load–frequency controller in a deregulated electric power system environment. In: Proceedings of the Conference on Decision & Control, USA, 1997. p. 3100–1.
[6] Bevrani H. A novel approach for power system load frequency controller design. In: Proceedings of IEEE-PES T&D Asia Pacific, Japan, 2002. p. 184–9.
[7] Arroyo JM, Conejo AJ. Optimal response of a power generator to energy, AGC, and reserve pool-based markets. IEEE Trans Power Syst 2002;17(2):404–10.
[8] Bakken BH, Grande OS. Automatic generation control in a deregulated power system. IEEE Trans Power Syst 1998;13(4):1401–6.
[9] Bevrani H, Rezazadeh A, Teshnehlab M. Comparison of existing LFC approaches in deregulated environment. In: Proceedings of 5th IEE International Conference on Power System Management and Control, UK, 2002. p. 238–43.
[10] Singh H, Paplexopoulos A. Competitive procurement of ancillary services by an independent system operator. IEEE Trans Power Syst 1999;14(2):498–504.
[11] Liu F, Song YH, Ma J, Mei S, Lu Q. Optimal load–frequency control in restructured power systems. IEE Proc Gener Transm Distrib 2003;150(1):87–95.
[12] Bevrani H, Mitani Y, Tsuji K. Robust load–frequency regulation in a new distributed generation environment. In: 2003 IEEE-PES General Meeting, Canada.
[13] Meliopoulos AS, Cokkinides GJ, Bakirtzis AG. Load–frequency control in a deregulated environment. Decision Support Syst 1999;24:243–50.
[14] Delfino B, Fornari F, Massucco S. Load–frequency control and inadvertent interchange evaluation in restructured power systems. IEE Proc Gener Transm Distrib 2002;149(5):607–14.

[15] Kumar J, Hoe NG, Sheble G. AGC simulator for price-based operation, Part 1: A model. IEEE Trans Power Syst 1997;2(12):527–32.
[16] Kumar J, Hoe NG, Sheble G. AGC simulator for price-based operation, Part 2: Case study results. IEEE Trans Power Syst 1997;2(12):533–8.
[17] Donde V, Pai MA, Hiskens IA. Simulation and optimization in a AGC system after deregulation. IEEE Trans Power Syst 2001;16(3):481–9.
[18] Khargonekar PP, Rotea MA. Mixed H_2/H_∞ control: a convex optimization approach. IEEE Trans Automat Control 1991;39:824–37.
[19] Scherer CW. Multiobjective H_2/H_∞ control. IEEE Trans Automat Control 1995;40:1054–62.
[20] Scherer CW, Gahinet P, Chilali M. Multiobjective output-feedback control via LMI optimization. IEEE Trans Automat Control 1997;42(7):896–911.
[21] Elgerd OI, Fosha C. Optimum megawatt-frequency control of multiarea electric energy systems. IEEE Trans Power Apparat Syst 1970;PAS-89(4):556–63.
[22] Fosha C, Elgerd OI. The megawatt-frequency control problem: a new approach via optimal control. IEEE Trans Power Apparat Syst 1970;PAS-89(4):563–77.
[23] Gahinet P, Nemirovski A, Laub AJ, Chilali M. LMI control toolbox. The MathWorks, Inc; 1995.